

Soft-Actuators in Cyclic Motion: Analytical Optimization of Stiffness and Pre-Load

Alexandra Velasco*, Gian Maria Gasparri[†], Manolo Garabini*, Lorenzo Malagia*, Paolo Salaris* and Antonio Bicchi*[†]

Abstract—In this paper, we study the role of soft actuation in the reduction of the energy cost for mechanical systems that perform cyclic tasks. The objective is to determine the optimal stiffness value and spring pre-load such that a given cost functional is minimized. For the analysis, we consider both fully actuated and underactuated mechanical systems using elastic actuators which, depending on how and where the springs are placed w.r.t. the actuator and the load, can be Series Elastic Actuators (SEAs) or Parallel Elastic Actuators (PEAs). The energy consumption depends not only on the actuation parameters but also on the trajectories followed to perform a given cyclic task. We show that the general problem in which both joint trajectories and actuation parameters are the optimization variables, can be cast as a simpler problem in which optimization regards only joint trajectories. Simulations of fully actuated and underactuated compliant robots are reported to demonstrate the effectiveness of the method. Although the stiffness optimization method is analytical in nature, it is directly applicable to existing systems whose model is unknown. A model-free experimental application on a prototype of a hopping robot with SEA is presented.

I. INTRODUCTION

A crucial component that dramatically affects performance of robots is their actuation. Recent developments in this field have introduced fixed or physically adjustable compliant elements to enrich the dynamics of conventional motors. These devices provide advantages w.r.t. rigid actuators, including higher peak performances, lower energy consumption and improved safety (see [1], [2], [3], [4]). This new tendency is the so called soft actuation, used for instance in manipulation [5], or in humanoid design [6].

Among soft actuators, SEAs [1] have a linear compliant element between a high impedance actuator and the load. On the other hand, PEAs have an elastic element in parallel with the motor (i.e. between two links). Other examples of soft actuators are the Variable Stiffness Actuators (VSA), and the Variable Impedance Actuators (VIA). VSAs have an elastic transmission whose stiffness can be mechanically adjusted, while VIAs can include mechanisms (e.g. brakes, dampers) allowing to change the output shaft impedance [7]. Recent studies explore the role of such devices in performance enhancement, looking at very dynamic tasks. For instance, in [8], [9] the objective is to optimally choose the stiffness to maximize the velocity of a VSA at a given final position with free final time. In [10], a new constraint is imposed, solving the same problem but with fixed terminal time.

The research leading to these results has received funding from the European Union Seventh Framework Programme under grants FP7 ICT-287513 “SAPHARI” project and the ERC Advanced Grant 291166 “SoftHands” project.

* Research Center “Enrico Piaggio”, University of Pisa, via Largo Lucio Lazzarino, 1, 56126 Pisa, Italy.

[†] Department of Advanced Robotics, Istituto Italiano di Tecnologia, via Morego, 30, 16163 Genova, Italy



Fig. 1. The prototype of the Hopper used for experiments.

In this paper, we study the role of soft actuation in the reduction of the energy cost for mechanical systems that perform cyclic tasks. The objective is to determine, for given desired joint trajectories, the optimal stiffness value and spring pre-load such that a given cost functional is minimized.

In the literature, several papers try to solve the same problem addressed in this work. For instance, a systematic method to optimally tune the joint stiffness of multi Degrees of Freedom (DoFs) SEA robots based on resonance analysis and energy storage maximization criteria is presented in [11]. A modal study was performed on the CoMAN (Compliant huMANoid) robot model, to derive the natural frequencies for different leg configurations during the single support walking phase. The joint stiffness was selected to set the resonances of the system, maximizing the energy stored in the joint springs. However, in [11], the design of trajectories is not based on joint stiffness selection directly and an approach to find the optimal stiffness and pre-load for the PEA case has not been addressed yet. Walking gaits generation for biped robots has also been addressed as a nonlinear optimization problem in [12]. The trajectories are obtained through cubic spline interpolation but joint compliance is not considered. In [13], an optimization is proposed to find feasible trajectories for a hopping robot. By constraining the problem, stable hopping of the rigid, underactuated robot is

achieved.

A control method for tracking cyclic trajectories is presented in [14], taking advantage of resonance of the dynamic systems and hence obtaining the optimal (constant, linear) stiffness value. In [15] an energy saving control method was applied to a simulated biped walking model. The link trajectories for a 4 DoF PEA robot are obtained via minimization of a performance index based on the squared torque. However, as in [14], the SEA case is not considered.

In this paper, we consider both fully actuated and underactuated dynamical systems using elastic actuation with either SEA or PEA providing an analytical methodology to optimize the actuation parameters for given joint trajectories. We show that the general problem in which both joint trajectories and actuation parameters have to be simultaneously optimized, can be translated into a problem in which the optimization would involve just the joint trajectories. However, in this paper the optimal characterization of the joint trajectories shape is not considered, showing only that, in case of sinusoidal trajectories the amplitude and the frequency play an important role in the reduction of the energy spent.

To show the effectiveness of the results we apply our method to a simple one-link robot manipulator tracking a sinusoidal joint trajectory and to a two-link robot manipulator performing a pick and place task. By several simulations, in both cases we show that the use of soft actuation allows to save energy w.r.t. the stiff actuation case. For the pick and place task, optimized soft actuation allows to save up to 53% of energy. Finally, a prototype of a hopping robot with SEAs is presented (see Fig. 1) and by experimentation we show that our method is applicable to existing systems whose model is unknown.

II. PROBLEM DEFINITION

This paper considers novel soft-robotics actuation schemes which may enhance performance of mechanical systems in cyclic tasks, i.e. reducing energy consumption, by exploiting the use of springs suitably placed on the system. For this reason, we study compliant mechanical systems which can be both fully actuated or underactuated. In the former case, there are as many actuators as Degrees of Freedom (DoF), whereas in the second one there are fewer control inputs than degrees of freedom [16].

Depending on how and where springs are placed on the system, the number of DoFs and the number of actuators, the dynamics of a mechanical system can assume particular forms as described in next subsections.

A. Fully Actuated Mechanical Systems

Let us first consider a fully actuated compliant mechanical system actuated by PEAs, e.g. a spring between two links for a serial manipulator (see Fig. 2(a)). For such a system, the number of DoFs remains equal to the number of actuators. Indicating by $q \in \mathbb{R}^n$ the generalized coordinates representing the configuration of the system and by $\tau \in \mathbb{R}^n$ the generalized torque provided by actuators, the dynamics can be written as

$$f(\ddot{q}, \dot{q}, q, t) = -K(q_e - q) + \tau, \quad (1)$$

where $q_e \in \mathbb{R}^n$ is the spring pre-load and $K \in \mathbb{R}^{n \times n}$ is the stiffness matrix. The term $f(\ddot{q}, \dot{q}, q, t)$ includes inertia, coriolis, and gravity terms.

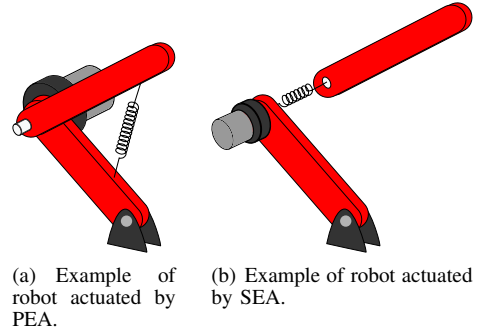


Fig. 2. Robot actuated by PEAs or SEAs.

B. Underactuated Mechanical Systems

Consider now the case in which the mechanical system is actuated by SEAs (see Fig. 2(b)), i.e. the springs between the actuator and the load (e.g. between the motor and the link for serial manipulators). Indicating by $\theta \in \mathbb{R}^n$ the motor positions and by J_m the inertia matrix of the motors, the dynamics can be written as

$$f(\ddot{q}, \dot{q}, q, t) = -K(q - \theta) \quad (2)$$

$$J_m \ddot{\theta} = K(q - \theta) + \tau, \quad (3)$$

Notice that the use of SEAs instead of PEAs increases the number of DoFs which become $2n$.

For particular mechanical systems there may be further DoFs which are not actuated, e.g. the position and orientation of humanoids w.r.t. a fixed reference frame. Let $x \in \mathbb{R}^m$ be those DoFs and assume the system is actuated by SEAs, the dynamics in this case can be written as

$$f_u(\ddot{x}, \dot{x}, x, \ddot{q}, \dot{q}, q, t) = 0 \quad (4)$$

$$f_a(\ddot{x}, \dot{x}, x, \ddot{q}, \dot{q}, q, t) = -K(q - \theta) \quad (5)$$

$$J_m \ddot{\theta} = K(q - \theta) + \tau, \quad (6)$$

where (4) represents the non-actuated dynamics, whereas (5) and (6) represent the underactuated dynamics.

Of course, if PEAs are used, the dynamics becomes

$$f_u(\ddot{x}, \dot{x}, x, \ddot{q}, \dot{q}, q, t) = 0 \quad (7)$$

$$f_a(\ddot{x}, \dot{x}, x, \ddot{q}, \dot{q}, q, t) = -K(q_e - q) + \tau. \quad (8)$$

C. Optimal Problem Formulation

In order to quantify the performance of the mechanical system and hence to determine optimal joint stiffness \hat{K} and/or pre-load \hat{q}_e values as well as optimal joint trajectories $q(t)$, we will consider two different cost functionals:

1) *Squared-Power index*: Assuming that the motor spends energy if the mechanical power is positive or negative, the cost functional of the whole mechanical system is

$$J_1 = \sum_{j=1}^n \int_0^T (\tau_j(t) \dot{\theta}_j(t))^2 dt, \quad (9)$$

where T represents the period of the cyclic task or its multiple.

2) *Squared-Torque index*: If the consumption is mainly related to the torque, then we can consider the cost

$$J_2 = \sum_{j=1}^n \int_0^T \tau_j^2(t) dt. \quad (10)$$

The optimal problem we are interested to solve is stated as follows:

$$\begin{aligned} \min_{\tau(t), \beta} J_i, \quad & i = 1, 2 \\ \text{s.t.} & \\ & \begin{cases} \text{Dynamics equations} \\ q(t) = q(t+T) \\ \xi_1(q, \dot{q}, \ddot{q}) \leq 0 \\ \xi_2(q, \dot{q}, \ddot{q}) = 0 \\ \beta_m \leq \beta \leq \beta_M \end{cases} \end{aligned} \quad (11)$$

where the dynamic equations can be those reported in subsection II-A in case of a fully actuated system with PEAs or those reported in subsection II-B for an underactuated system with SEAs or PEAs. β is a vector containing joint stiffness K and pre-load q_e in case of PEAs and only stiffness K in case of SEAs. These values have limits $\beta_M = [K_M, q_{e,M}]$ and $\beta_m = [K_m, q_{e,m}]$. T is the period of the cyclic task which translates in requiring that $q(t) = q(t+T)$. Moreover, the nonlinear constraints ξ_1 and ξ_2 which depend on variable q , \dot{q} and \ddot{q} , define the task. For instance, in a pick and place task for a two-link planar manipulator, we can constrain the motion of the end-effector to the line between two points.

III. OPTIMIZATION OF STIFFNESS AND PRE-LOAD PARAMETERS

In this section we will exploit the dynamic equations of the mechanical system at hand in order to write the cost functional as a function of joint trajectories $q(t)$ (and their derivatives) and actuation parameters β . It is important to note that in the following analysis we assume that $K = \text{diag}[K_1, K_2, \dots, K_n]$ and $J_m = \text{diag}[J_{m1}, J_{m2}, \dots, J_{mn}]$.

At the end we will be able to determine the optimal stiffness and pre-load values as functions of given desired trajectories $q_d(t)$ and hence to translate the optimal problem given in (11) in a simpler problem where the objective is only to find the optimal joint trajectories.

A. Stiffness optimization for a mechanical system using SEAs.

Let us assume that joint trajectories $q(t) = q_d(t)$ and its first $\dot{q}(t) = \dot{q}_d(t)$ and second $\ddot{q}(t) = \ddot{q}_d(t)$ derivatives are given, and consider a mechanical system as in (4), (5) and (6). By integration, from (4) it is possible to find x as a function of the desired trajectories $q_d(t)$ and hence, by substituting in (5) and (6), to obtain

$$f(\ddot{q}_d, \dot{q}_d, q_d, t) = -K(q_d - \theta) \quad (12)$$

$$J_m \ddot{\theta} = K(q_d - \theta) + \tau, \quad (13)$$

which is in the form represented by (2) and (3). Hence, the following analysis is valid for every underactuated system using SEAs.

As matrices K and J_m are assumed to be diagonal, (12) and (13) can be written for each actuator as

$$f_j(\ddot{q}_d, \dot{q}_d, q_d, t) = -K_j[q_{d,j} - \theta_j], \quad (14)$$

$$J_{m,j} \ddot{\theta}_j = \tau_j + K_i(q_{d,j} - \theta_j), \quad (15)$$

for $j = 1, 2, \dots, n$, where $f_j(\ddot{q}_d, \dot{q}_d, q_d, t)$ denotes the j -th element of the function $f(\ddot{q}_d, \dot{q}_d, q_d, t)$. From (14) we have

$$\theta_j = K_j^{-1} f_j(\ddot{q}_d, \dot{q}_d, q_d, t) + q_{d,j}, \quad (16)$$

$$\dot{\theta}_j = K_j^{-1} \dot{f}_j(\ddot{q}_d, \dot{q}_d, q_d, t) + \dot{q}_{d,j}, \quad (17)$$

$$\ddot{\theta}_j = K_j^{-1} \ddot{f}_j(\ddot{q}_d, \dot{q}_d, q_d, t) + \ddot{q}_{d,j}. \quad (18)$$

Replacing (16) and (18) in (15), the j -th motor torque required to track the desired trajectory $q_d(t)$ is

$$\tau_j = J_{m,j} (K_j^{-1} \ddot{f}_j(\ddot{q}_d, \dot{q}_d, q_d, t) + \ddot{q}_{d,j}) + f_j(\ddot{q}_d, \dot{q}_d, q_d, t). \quad (19)$$

We rewrite cost index J_1 in terms of $q_d(t)$, $\dot{q}_d(t)$ and stiffness K . The j -th element related to the j -th actuator is

$$J_{1,j} = \int_0^T (\tau_j(t) \dot{\theta}_j(t))^2 dt. \quad (20)$$

By substituting (17) and (19) in (20), we obtain

$$\begin{aligned} J_{1,j} &= \int_0^T (\tau_j(t) \dot{\theta}_j(t))^2 dt = \\ &= \int_0^T ((J_{m,j} K_j^{-1} \ddot{f}_j + J_{m,j} \ddot{q}_{d,j} + f_j)(K_j^{-1} \dot{f}_j + \\ &\quad + \dot{q}_{d,j}))^2 dt = \int_0^T \left(\frac{a_j(t)}{K_j^2} + \frac{b_j(t)}{K_j} + c_j(t) \right)^2 dt \end{aligned}$$

where $a_j(t) = J_{m,j} \ddot{f}_j \dot{f}_j$, $b_j(t) = J_{m,j} (\ddot{f}_j \dot{q}_{d,j} + \dot{f}_j \ddot{q}_{d,j}) + f_j \dot{f}_j$ and $c_j(t) = J_{m,j} \dot{q}_{d,j} \dot{q}_{d,j} + \dot{f}_j \dot{q}_{d,j}$.

Notice that $J_{1,j}$ depends only on the stiffness K_j of the j -th actuator. Hence,

$$\min_K J_1 = \sum_j \min_{K_j} J_{1,j}.$$

The optimal solution for each K_j is such that $\frac{\partial J_{1,j}}{\partial K_j} = 0$, which, after some algebra, becomes

$$4A_{S,j} + 3K_j B_{S,j} + 2C_{S,j} K_j^2 + D_{S,j} K_j^3 = 0, \quad (21)$$

where

$$A_{S,j} = \int_0^T a_j^2(t) dt, \quad B_{S,j} = \int_0^T 2a_j(t) b_j(t) dt$$

$$C_{S,j} = \int_0^T (2a_j(t) c_j(t) + b_j^2(t)) dt$$

$$D_{S,j} = \int_0^T 2b_j(t) c_j(t) dt, \quad E_{S,j} = \int_0^T c_j^2(t) dt.$$

Notice that $A_{S,j}$, $B_{S,j}$, $C_{S,j}$, $D_{S,j}$ and $E_{S,j}$ depends only on $q_{d,j}$, $\dot{q}_{d,j}$ and $\ddot{q}_{d,j}$ which are assumed known.

For the cost functional J_2 , the j -th element related to the j -th actuator is

$$J_{2,j} = \int_0^T \tau_j^2(t) dt.$$

and after substituting (19), with some algebra, we obtain

$$J_{2,j} = \frac{F_{S,j}}{K_j^2} + \frac{G_{S,j}}{K_j} + H_{S,j},$$

where

$$F_{S,j} = \int_0^T (J_{m,j} \ddot{f}_j)^2 dt, \quad H_{S,j} = \int_0^T (J_{m,j} \ddot{q}_{d,j} + f_j)^2 dt,$$

$$G_{S,j} = \int_0^T 2J_{m,j} \dot{f}_j (J_{m,j} \ddot{q}_{d,j} + f_j) dt.$$

Also in this case $J_{2,j}$ depends only on the stiffness K_j of the j -th actuator. Hence,

$$\min_K J_2 = \sum_j \min_{K_j} J_{2,j}.$$

The optimal solution for each K_j is such that $\frac{\partial J_{2,j}}{\partial K_j} = 0$, obtaining

$$\hat{K}_j = -2 \frac{F_{S,j}}{G_{S,j}}. \quad (22)$$

B. Stiffness and pre-load optimization for a mechanical system using PEAs

Let us assume also in this case given desired trajectories $q(t) = q_d(t)$ for the joints and its derivatives, and consider a mechanical system as in (7) and (8). By integration, from (7) it is possible to find x as a function of the desired trajectories $q_d(t)$ and hence, by substituting in (8) to obtain

$$f(\ddot{q}_d, \dot{q}_d, q_d, t) = -K(q_e - q_d) + \tau, \quad (23)$$

which is equivalent to the mechanical system represented by (1). Hence, the following analysis is valid for every underactuated or fully actuated system using PEAs.

Because of the assumption on stiffness matrix K , (23) can be written for each actuator as

$$f_j(\ddot{q}_d, \dot{q}_d, q_d, t) = -K_j(q_{e,j} - q_{d,j}) + \tau_j, \quad (24)$$

for $j = 1, 2, \dots, n$, where $f_j(\ddot{q}_d, \dot{q}_d, q_d, t)$ denotes the j -th element of the function $f(\ddot{q}_d, \dot{q}_d, q_d, t)$.

From (24), we have

$$\tau_j = f_j + K_j(q_{e,j} - q_{d,j}). \quad (25)$$

Recalling index J_1 using PEA, for the j -th actuator, we have

$$J_{1,j} = \int_0^T (\tau_j(t) \dot{q}_{d,j}(t))^2 dt.$$

By substituting (25) in previous expression of $J_{1,j}$ we obtain

$$J_{1,j} = A_{P,j} - K_j q_{e,j} B_{P,j} +$$

$$+ K_j C_{P,j} + K_j^2 q_{e,j}^2 D_{P,j} +$$

$$- K_j^2 q_{e,j} E_{P,j} + K_j^2 F_{P,j}.$$

where

$$A_{P,j} = \int_0^T f_j^2 \dot{q}_{d,j}^2 dt, \quad B_{P,j} = \int_0^T 2f_j \dot{q}_{d,j}^2 dt,$$

$$C_{P,j} = \int_0^T 2f_j \dot{q}_{d,j}^2 q_{d,j} dt, \quad D_{P,j} = \int_0^T \dot{q}_{d,j}^2 dt,$$

$$E_{P,j} = \int_0^T 2\dot{q}_{d,j}^2 q_{d,j} dt, \quad F_{P,j} = \int_0^T \dot{q}_{d,j}^2 q_{d,j}^2 dt.$$

For given desired trajectories $q_{d,j}$, $J_{1,j}$ depends only on K_j and $q_{e,j}$. Hence,

$$\min_{K,q_e} J_1 = \sum_j \min_{K_j, q_{e,j}} J_{1,j}.$$

The optimal actuation parameters are such that

$$\frac{\partial J_{1,j}}{\partial K_j} = 0, \quad \frac{\partial J_{1,j}}{\partial q_{e,j}} = 0, \quad (26)$$

which become

$$-B_{P,j} q_{e,j} + C_{P,j} + 2D_{P,j} K_j q_{e,j}^2 +$$

$$-2E_{P,j} K_j q_{e,j} + 2F_{P,j} K_j = 0 \quad (27)$$

$$-B_{P,j} K_j + 2D_{P,j} K_j^2 q_{e,j} - E_{P,j} K_j^2 = 0. \quad (28)$$

Solving previous equations for K and $q_{e,j}$, we obtain

$$\hat{K}_j = \frac{B_{P,j} E_{P,j} - 2C_{P,j} D_{P,j}}{4D_{P,j} F_{P,j} - E_{P,j}^2} \quad (29)$$

$$\hat{q}_{e,j} = \frac{C_{P,j} E_{P,j} - 2B_{P,j} F_{P,j}}{2C_{P,j} D_{P,j} - B_{P,j} E_{P,j}} \quad (30)$$

For the cost functional J_2 , after substituting (25), we can obtain

$$J_{2,j} = G_{P,j} - K_j q_{e,j} H_{P,j} + K_j I_{P,j} +$$

$$+ T K_j^2 q_{e,j}^2 + K_j^2 L_{P,j} - K_j^2 q_{e,j} M_{P,j}, \quad (31)$$

where

$$G_{P,j} = \int_0^T f_j^2(t) dt, \quad H_{P,j} = \int_0^T 2f_j(t) dt,$$

$$I_{P,j} = \int_0^T 2f_j(t) q_{d,j}(t) dt, \quad L_{P,j} = \int_0^T \dot{q}_{d,j}^2(t) dt,$$

$$M_{P,j} = \int_0^T 2q_{d,j}(t) dt$$

Notice that, $J_{2,j}$ depends only on K_j and $q_{e,j}$, hence

$$\min_{K,q_e} J_2 = \sum_j \min_{K_j, q_{e,j}} J_{2,j}.$$

The optimal actuation variables for a given desired trajectory $q_{d,j}$ can be obtained by solving $\frac{\partial J_{2,j}}{\partial q_{e,j}} = 0$ and $\frac{\partial J_{2,j}}{\partial K_j} = 0$, which become

$$-q_{e,j} H_{P,j} + I_{P,j} + 2K_j q_{e,j}^2 T +$$

$$+ 2K_j L_{P,j} - 2K_j q_{e,j} M_{P,j} = 0$$

$$-K_j H_{P,j} + 2K_j^2 q_{e,j} T - K_j^2 M_{P,j} = 0.$$

Finally, solving for K and $q_{e,j}$, we obtain

$$\hat{K}_j = \frac{\hat{q}_{e,j} H_{P,j} - I_{P,j}}{2(\hat{q}_{e,j}^2 T + L_{P,j} - \hat{q}_{e,j} M_{P,j})} \quad (32)$$

$$\hat{q}_{e,j} = \frac{H_{P,j} + \hat{K}_j M_{P,j}}{2\hat{K}_j T}. \quad (33)$$

Table I summarizes the expressions for the optimal actuation parameters.

The optimal value for stiffness K and pre-load q_e obtained before are not necessarily inside the admissible range of values. In this case, the optimal values are on the boundary of the admissible set for the actuation parameters.

	J_1	J_2
SEA	A solution of (21)	$\hat{K}_j = -2 \frac{F_{S,j}}{G_{S,j}}$
PEA	$\hat{K}_j = \frac{B_{P,j} E_{P,j} - 2C_{P,j} D_{P,j}}{4D_{P,j} F_{P,j} - E_{P,j}^2}$	$\hat{K}_j = \frac{\hat{q}_{e,j} H_{P,j} - I_{P,j}}{2(\hat{q}_{e,j}^2 T + L_{P,j} - \hat{q}_{e,j} M_{P,j})}$
	$\hat{q}_{e,j} = \frac{C_{P,j} E_{P,j} - 2B_{P,j} F_{P,j}}{2C_{P,j} D_{P,j} - B_{P,j} E_{P,j}}$	$\hat{q}_{e,j} = \frac{H_{P,j} + \hat{K}_j M_{P,j}}{2\hat{K}_j T}$

TABLE I
OPTIMAL PARAMETERS \hat{K} AND \hat{q}_e .

For the SEA, cost functional J_2 has a unique global minimum and hence, if such value is not admissible, then

$$\hat{K} = \begin{cases} K_m & \text{if } J_i(K_m) < J_i(K_M) \\ K_M & \text{if } J_i(K_M) < J_i(K_m). \end{cases} \quad (34)$$

On the other hand, for cost functional J_1 , the optimal stiffness value can be obtained solving (21) which has three solutions. Hence, the optimal stiffness can be one of these solutions or it can lie on the border of the admissible range of values.

For PEA, the performance index depends on the two optimization variables K and q_e . However, both cost functionals have a unique global minimum. Hence, if the optimal values are such that $\hat{K} \notin [K_m, K_M]$ and/or $\hat{q}_e \notin [q_{e,m}, q_{e,M}]$, then the optimal parameters are in the border of the admissible range of values. Consider the following cases:

- 1) if $\hat{K} \notin [K_m, K_M]$ and $\hat{q}_e \in [q_{e,m}, q_{e,M}]$. In this case, if the first of (26) is satisfied by \hat{q}_e ,

$$\hat{K} = \begin{cases} K_m & \text{if } J(K_m, \hat{q}_e(K_m)) < J(K_M, \hat{q}_e(K_m)), \\ K_M & \text{if } J(K_M, \hat{q}_e(K_M)) < J(K_m, \hat{q}_e(K_M)); \end{cases}$$

- 2) $\hat{K} \in [K_m, K_M]$ and $\hat{q}_e \notin [q_{e,m}, q_{e,M}]$. In this case, if the second of (26) is satisfied by \hat{K} ,

$$\hat{q}_e = \begin{cases} q_{e,m} & \text{if } J(\hat{K}(q_{e,m}), q_{e,m}) < J(\hat{K}(q_{e,M}), q_{e,m}) \\ q_{e,M} & \text{if } J(\hat{K}(q_{e,M}), q_{e,M}) < J(\hat{K}(q_{e,m}), q_{e,m}); \end{cases}$$

- 3) $\hat{K} \notin [K_m, K_M]$ and $\hat{q}_e \notin [q_{e,m}, q_{e,M}]$, then the optimal pair \hat{K}, \hat{q}_e is related to the minimum value among the following: $J(K_m, q_{e,M})$, $J(K_M, q_{e,M})$, $J(K_m, q_{e,m})$ and $J(K_M, q_{e,m})$.

With the procedure followed so far, we have obtained a simpler problem in which only the joint trajectories are the optimization variables which can not be achieved analytically. Hence, in next sections we provide numerical solution applying our method to some mechanical systems.

IV. SIMULATION RESULTS

Consider some cases of fully actuated and underactuated systems by simulations.

A. One-link Robot manipulator

First, consider a one-link manipulator, actuated by a SEA or a PEA, which performs a cyclic task. The dynamic of this mechanical system can be written as

$$\begin{aligned} M\ddot{q} + c\dot{q} + mgL \cos q + K(q - \theta) &= 0 \\ J_m\ddot{\theta} + K(\theta - q) &= \tau \end{aligned} \quad (35)$$

in case of SEA, and

$$M\ddot{q} + c\dot{q} + mgL \cos q + K(q - q_e) = \tau \quad (36)$$

in case of PEA. $M = mL^2 + I$, L is the length of the link, m is the load at the end of the link, I the inertia of the link and c is the damping. Assume that in both cases, the joint trajectory is given as $q_d(t) = B + A \sin(\omega t)$, where the amplitude A , the frequency ω , and the angle B around which the link oscillates, depend on the task.

a) *PEAs*: The problem of finding optimal stiffness and pre-load can be solved analytically. Indeed, substituting $q_d(t)$, $\dot{q}_d(t)$ and $\ddot{q}_d(t)$ in (36), we can obtain τ and substitute it in J_1 . The minimum of J_1 is achieved with

$$\begin{aligned} \hat{K} &= \omega^2 M + \frac{8mgLB_J(2, A) \sin B}{A^2} \\ \hat{q}_e &= B + \frac{2gmLAB_J(1, A) \cos B}{A^2 \omega^2 M + 8mgLB_J(2, A) \sin B}, \end{aligned}$$

where $B_J(n, x)$ is the Bessel function. Notice that for small amplitudes, i.e. $A \rightarrow 0$, $\frac{8B_J(2, A)}{A^2} \rightarrow 1$, the optimal stiffness becomes $\hat{K} = \omega^2 M + mgL \sin B$ which corresponds to the resonant condition for the linearized system in $q = B$.

For the cost functional J_2 , the minimum is obtained with

$$\begin{aligned} \hat{K} &= \omega^2 M + \frac{2mgLB_J(1, A) \sin B}{A} \\ \hat{q}_e &= B + \frac{AmgLB_J(0, A) \cos B}{A^2 \omega^2 M + 2mgLB_J(1, A) \sin B}. \end{aligned}$$

Also in this case, for small amplitudes, the optimal stiffness becomes $\hat{K} = \omega^2 M + mgL \sin B$ which corresponds to the resonant condition for the linearized system in $q = B$. Of course, for the nonlinear system, the cost function obtained by using the optimal parameters assumes a bigger value but $|\tau|$ achieves the minimum value. This is similar to the resonance concept of linear systems.

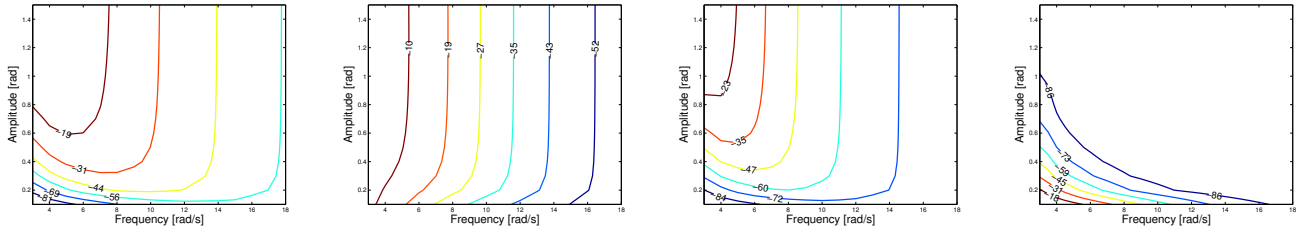
Finally, for a given B , the optimal values for \hat{K} obtained by using J_1 and J_2 are quite similar. In particular, if $B = 0$ and for any amplitude A , $\hat{K} = \omega^2 M$, i.e. the value of stiffness corresponding to the resonant condition for the linearized system in $q = 0$. The pre-load are different but from a quantitative point of view are quite similar, depending mainly on B .

b) *SEAs*: The problem of finding optimal stiffness can be solved analytically only in case of J_2 as cost functional. Indeed, solving the first equation of (35) for θ and substituting it, with its second derivative in the second equation of (35), we obtain τ and substituting it in J_2 , with $\dot{\theta}(t) = K^{-1}(M\ddot{q}_d(t) + c\dot{q}_d(t) + mgL \cos q_d(t)) + q_d(t)$, the minimum can be achieved in closed form. The expression is complicated and can not be reported here. However, in case of $B = 0$, $d = 0$ and for small amplitudes, the optimal value is

$$\hat{K} = \frac{MJ_m \omega^2}{(M + J_m)},$$

which corresponds to resonant condition for the linearized system around $q = 0$, without losses ($d = 0$).

In case of J_1 , the optimal stiffness and the corresponding value of the cost functional can be only obtained numerically. For a comparison between PEA and SEA in terms of efficiency, and to underline the advantage of soft w.r.t. stiff actuation, in Fig. 3 we report the cost saving in terms of J_1 and J_2 in case of PEAs or SEAs w.r.t. the stiff case. In particular, Fig. 3(a) and 3(b) show the energy saving using



(a) Energy saving in terms of J_1 for PEAs. (b) Energy saving in terms of J_1 for SEAs. (c) Energy saving in terms of J_2 for PEAs. (d) Energy saving in terms of J_2 for SEAs.

Fig. 3. Energy saving (in % w.r.t. the stiff case) for a one-link robot manipulator, varying the amplitude A and the frequency ω of the desired joint trajectory $q_d(t) = A \sin(\omega t) + B$, with $B = 0$.

J_1 as measure. On the other hand, Fig. 3(c) and 3(d) show the energy saving using J_2 as measure.

In particular, considering Fig. 3(a) and 3(c), the use of PEAs permit to get as much more saving as the amplitude and the frequency of the desired trajectory decrease, independently from the cost functional used, i.e. J_1 or J_2 . However, we have a consistent saving also in case of large values of frequency, independently from the amplitude.

Differently, in case of SEA, savings depend on the cost functional we consider. In terms of J_1 , consistent savings can be obtained increasing the frequency. The amplitude significantly influence only for small values. In terms of J_2 , consistent savings can be obtained for small values of the amplitude and large values of frequency or for large values of the amplitude and small values of frequency.

From another point of view, we can conclude that, in terms of J_2 , PEA is more convenient for small amplitudes at low frequency or large amplitudes at high frequency, while SEA is more convenient for small amplitudes at high frequency or for large amplitudes at low frequency. In terms of J_1 , we can observe differences w.r.t. J_2 only in case of SEA. Indeed, SEA becomes convenient only for high frequencies, independently from the amplitude.

B. Two-link robot manipulator

Let us consider now a two-link robot manipulator which performs a pick and place task. The robot moves on a horizontal plane. In case of PEAs, we have a fully actuated mechanical system (2 motors and 2 DoFs), whereas in case of SEAs an under-actuated one (2 motors and 4 DoF). $q_{1,d} = A_1 \sin(\omega t) + B_1$ and $q_{2,d} = A_2 \sin(\omega t) + B_2$ are the desired joint trajectories. The robot moves from a given initial position Q_1 to a given final position Q_2 . The values of the amplitudes A_1 and A_2 , as well as the angle B_1 and B_2 around which each link moves, depend on these positions. Of course, for any couple of point Q_1 and Q_2 , these parameters are univocally determined by inverse kinematics. For this problem, we have performed several simulations applying our methodology. Some of them are reported in Fig. 4, which shows the values of cost functionals J_1 and J_2 in case of PEAs and SEAs, as well as the optimal parameters (stiffness and/or pre-load) for different values of frequency ω . Moreover, cost functionals J_1 and J_2 for the same tasks for the stiff case are also reported. Notice that for all cases reported in Figure 4, the cost functionals assume the minimum values.

For all cases, it is shown in Fig. 4 that the stiff actuation is the most expensive in terms of energy spent. Furthermore,

in the first two cases (a. and b.), when using J_1 , PEA gives the lowest cost, while for the other two cases (c. and d.) the best performance is achieved when using SEA. The same happens for J_2 . The optimal joint stiffness is higher as ω increases. Moreover, for the SEA case, the spring in the first joint should be stiffer than the second joint, while for the PEA case, the spring for the first joint should be softer than the second one. Results evidence that elastic actuators allow to save energy. Indeed, at the highest frequency used in these simulations, the energy savings in terms of cost functional J_1 is up to 90% w.r.t. the rigid case in the SEA and PEA cases. In terms of J_2 , at the same frequency, the energy savings is up to 62% in case of SEAs and 23% in case of PEAs, w.r.t. the rigid case. In Fig. 4 is also reported values of the optimal pre-load values q_e for the PEA case. Notice that this value is constant for all cases except for the cases a. and b. where the optimal pre-load value of the second joint changes with frequency.

V. MODEL-FREE APPLICATION

In this section we present an experimental application on a prototype of the hopping robot represented in Fig. 1. The objective is to show that, even though the proposed method is analytical, it is directly applicable to existing systems whose model is not accurate or not available at all. Indeed, the optimization of the actuation parameters need to evaluate the function $f_a(\ddot{x}, \dot{x}, x, \dot{q}, \ddot{q}, q, t)$ and in (5) in case of SEA, or in (8) in case of PEA, in terms of the desired joint trajectories. However, in an experimental setup, as $f_a(\cdot)$ can also be directly measured from the real system by means of suitable sensors. To correctly the optimization procedure, it is sufficient to obtain the derivatives of the measured signal $f_a(t)$, which can be obtained by applying techniques such as e.g. in [17]. Through the following experiment we are hence able to show that our method can be applied to systems whose model is unknown, i.e. in a model-free fashion.

The prototype of the planar elastic hopping robot represented in Fig. 1. Referring to Fig. 5, it has one leg which is composed of two links (1 and 2), three DoFs and it is linked to the frame through two non actuated DoFs (3 and 4). All joints are provided with a contactless magnetic rotary position sensor (AS5045¹, colored in red). The two joints of the leg are actuated by DC geared motors (maxon DCX 22S² with graphite brushes 24 V, and planetary gearhead GPX22 with reduction ratio 83 : 1, 5 and 6). The hopper is actuated

¹<http://www.ams.com>

²<http://dcx.maxonmotor.com>

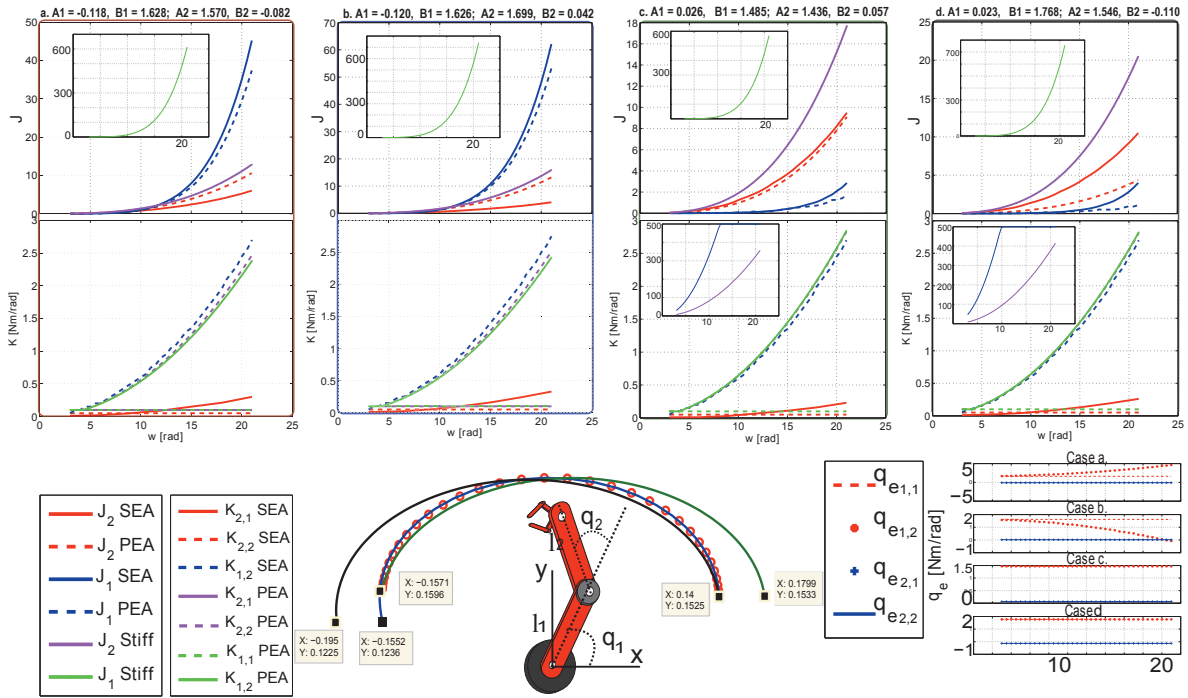


Fig. 4. The dynamics parameters used are: link masses $m_1 = m_2 = 0.84$ kg; link lengths $l_1 = 0.14$ m, $l_2 = 0.165$ m; motor inertias $J_{m_1} = J_{m_2} = 10^{-5}$ kgm^2 , link inertias $J_1 = 3.96 \cdot 10^{-4}$ kgm^2 , $J_2 = 5.29 \cdot 10^{-4}$ kgm^2 w.r.t. centroid. The red, blue, green and black curves on the center of the figure show the desired end-effector trajectories. The corresponding results of cost functionals and optimal stiffness are shown in the boxes of the same color (a. to d. from left to right). The figure legends are indicated below the boxes. For cases a. and b. (red and blue), $\hat{K}_{(1,1)SEA} = 500$ Nm/rad so it is not shown; for cases c. and d. (green and black) it is indicated with blue continuous line. The pre-load optimization results for the PEA case are shown at bottom right.

by a SEA in the knee, while the other joint is stiff (see Fig. 5). The series elastic transmission 10 between the actuator 11 and the knee joint is composed of two rubber bands.

Wheel 7 is placed at the extremity of the leg in order to reduce the effect of the friction component perpendicular to the direction of motion. To guarantee a vertical hopping, the leg has been constrained through a vertical linear guide 8. An electronic board³ 9 has been used to acquire the measurements from the encoders and to implement a closed loop position control scheme tracking the desired trajectories (the controller furnishes input values at a frequency of 1 kHz).

The stiffness of the equivalent torsional spring between the knee link and the actuator has been experimentally determined by applying different value of torques and the corresponding deformations (see Fig. 5, Stiffness identification). Once the stiffness value is known (~ 0.58 Nm/rad), sinusoidal reference signals that guarantee a stable hopping have been imposed to the motors (black lines in Fig. 5). During the experiment (see the attached video), we have recorded data provided by encoders (red and blue lines in Fig. 5), and hence the signal $f_a(t)$ in (5) in case of SEA, or (8) in case of PEA. Having the signal $f_a(t)$, it is possible to apply our method to determine, for those link trajectories, the values of cost functional J_1 and J_2 for different values of K and, for PEA, the corresponding best value of q_e , as reported in Fig. 6.

For both indices the best result in terms of energy saving can be obtained for SEAs by setting $K \approx 0.6$ Nm/rad as

stiffness value. Notice that, this value is quite similar to that obtained by the stiffness identification procedure. Hence, if the controller is able to guarantee the same joint trajectories used in the optimization phase, with any other value of stiffness, the energy spent would increase.

VI. CONCLUSIONS AND FUTURE WORK

In this paper, we have studied the role of soft actuation in the reduction of the energy cost for mechanical systems that perform cyclic tasks. We have considered both SEAs and PEAs and determined the optimal stiffness value and spring pre-load such that a given cost functional is minimized. We have shown that the energy consumption also depends on the shape of the joint trajectories used to perform a given cyclic task. In this paper the desired joint trajectories are sinusoids which may not guarantee the best behavior in terms of energy saving. Future works will be dedicated to explore the role of the shape of the joint trajectories in the reduction of the energy cost as well as how to design them.

Moreover, results obtained in this paper can be applied directly to more complex systems such as hopping or humanoid robots for which soft actuation can be exploited to achieve a reduction of the so called ‘‘Cost of Transport’’ which is an important aspect of these robots. Future works will be dedicated to show by experimentation the reduction of the energy consumption.

VII. ACKNOWLEDGMENT

Authors gratefully acknowledge Felipe Belo, Fabio Bonomo, Manuel Giuseppe Catalano, Manuel Bonilla,

³<http://www.naturalmotioninitiative.com/>

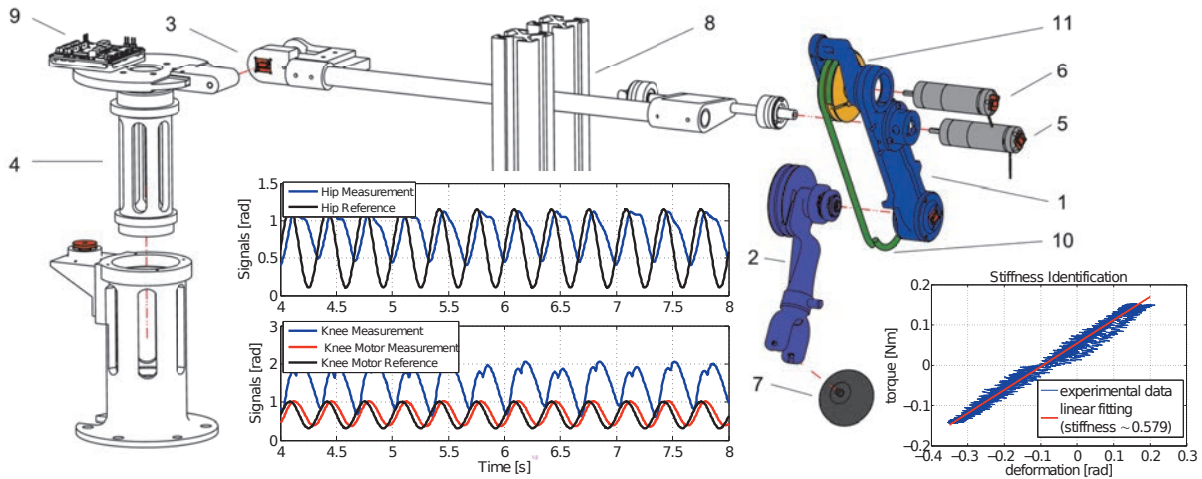
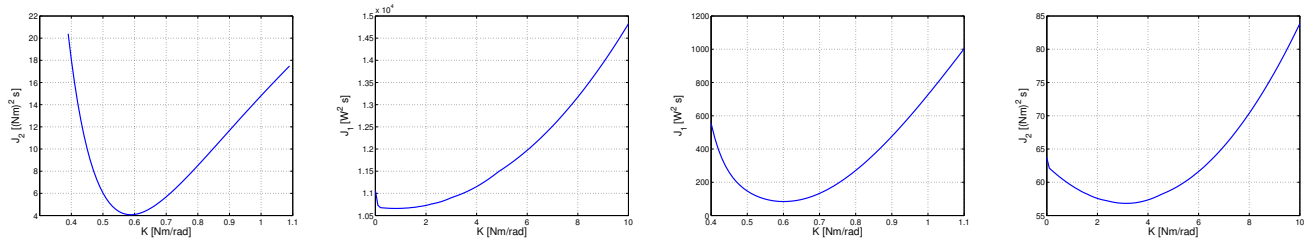


Fig. 5. Exploded 3D view of the hopping robot. The figure also shows the graphical values of torque and corresponding deformation used for stiffness identification. Moreover, in the center of the picture are reported reference signals and measured link trajectories.



(a) Cost index J_2 for different values stiffness in case of SEAs. (b) Cost index J_2 for different values stiffness in case of PEAs. (c) Cost index J_1 for different values stiffness in case of SEAs. (d) Cost index J_1 for different values stiffness in case of PEAs.

Fig. 6. Cost indices J_1 and J_2 for different values of K . In the PEA case, for each value of stiffness, the corresponding value of the cost functional is computed by using the best value of \hat{q}_e .

Kamilo Melo, Alessandro Serio and Andrea Di Basco for their assistance in the prototype design.

REFERENCES

- [1] G. Pratt and M. Williamson, "Series elastic actuators," in *Intelligent Robots and Systems 95. 'Human Robot Interaction and Cooperative Robots', Proceedings. 1995 IEEE/RSJ International conference on*, vol. 1, aug 1995, pp. 399–406 vol.1.
- [2] B. Vanderborght, B. Verrelst, R. V. Ham, M. V. Damme, D. Lefeber, B. M. Y. Duran, and P. Beyl, "Exploiting natural dynamics to reduce energy consumption by controlling the compliance of soft actuators," *I. J. Robotic Res.*, vol. 25, no. 4, pp. 343–358, 2006.
- [3] M. Catalano, G. Grioli, M. Garabini, F. Bonomo, M. Mancinit, N. Tsagarakis, and A. Bicchi, "Vsa-cubebot: A modular variable stiffness platform for multiple degrees of freedom robots," in *Robotics and Automation (ICRA), 2011 IEEE International Conference on*, may 2011, pp. 5090–5095.
- [4] M. D. Taylor, "A compact series elastic actuator for bipedal robots with human-like dynamic performance," Master's thesis, Robotics Institute, Carnegie Mellon University, August 2011.
- [5] A. Albu-Schaffer, O. Eiberger, M. Grebenstein, S. Haddadin, C. Ott, T. Wimbock, S. Wolf, and G. Hirzinger, "Soft robotics," *Robotics Automation Magazine, IEEE*, 2008.
- [6] N. G. Tsagarakis, M. Laffranchi, B. Vanderborght, and D. Caldwell, "A compact soft actuator unit for small scale human friendly robots," in *Robotics and Automation, 2009. ICRA '09. IEEE International Conference on*, 2009.
- [7] M. G. Catalano, G. Grioli, M. Garabini, F. A. W. Belo, A. di Basco, N. G. Tsagarakis, and A. Bicchi, "A variable damping module for variable impedance actuation," in *International Conference of Robotics and Automation - ICRA 2012, Saint Paul, MN, USA, May 14 - 18 2012*.
- [8] J.-J. Park, S. Haddadin, J.-B. Song, and A. Albu-Schaffer, "Designing optimally safe robot surface properties for minimizing the stress characteristics of human-robot collisions," in *Robotics and Automation (ICRA), 2011 IEEE International Conference on*, 2011.
- [9] M. Garabini, A. Passaglia, F. Belo, P. Salaris, and A. Bicchi, "Optimality principles in variable stiffness control: The vsa hammer," in *Intelligent Robots and Systems (IROS), 2011 IEEE/RSJ International Conference on*, 2011.
- [10] M. G. Catalano, G. Grioli, M. Garabini, F. A. W. Belo, A. di Basco, N. Tsagarakis, and A. Bicchi, "Implementing a variable impedance actuator," in *International Conference of Robotics and Automation - ICRA 2012, Saint Paul, MN, USA, May 14 - 18 2012*, pp. 2666–2672.
- [11] N. Tsagarakis, S. Morfeý, G. Cerda, Z. Li, and D. G. Caldwell, "Compliant humanoid coman: Optimal joint stiffness tuning for modal frequency control," in *International Conference on Robotics and Automation*, 2013.
- [12] A. Werner, R. Lampariello, and C. Ott, "Optimization-based generation and experimental validation of optimal walking trajectories for biped robots," in *Intelligent Robots and Systems (IROS), 2012 IEEE/RSJ International Conference on*, 2012.
- [13] T.-Y. Wu, T. J. Yeh, and B.-H. Hsu, "Trajectory planning of a one-legged robot performing stable hop," in *Intelligent Robots and Systems (IROS), 2010 IEEE/RSJ International Conference on*, 2010.
- [14] M. Uemura and S. Kawamura, "Resonance-based motion control method for multi-joint robot through combining stiffness adaptation and iterative learning control," in *Proceedings of the 2009 IEEE international conference on Robotics and Automation*, ser. ICRA'09, 2009.
- [15] M. Uemura, K. Kimura, and S. Kawamura, "Generation of energy saving motion for biped walking robot through resonance-based control method," in *IROS. IEEE*, 2009, pp. 2928–2933.
- [16] M. W. Spong, "Underactuated mechanical systems," in *Control Problems in Robotics and Automation*. Springer-Verlag, 1998.
- [17] M. Fliess and H. Sira-Ram, "State reconstructors: a possible alternative to asymptotic observers and kalman filters," in *Computation Engineering in Systems Applications, CESA*, 2003.